Journal of Electronic Materials (2022) 51:4063–4072
https://doi.org/10.1007/s11664-022-09643-2

ORIGINAL RESEARCH ARTICLE

Predicting the Cu_6Sn_5 Growth Kinetics During Thermal Aging of Cu-Sn Solder Joints Using Simplistic Kinetic Modeling

Ankita Roy[1] · Amey Luktuke[2] · Nikhilesh Chawla[2] · Kumar Ankit[1]

Received: 25 January 2022 / Accepted: 5 April 2022 / Published online: 11 May 2022

Abstract

Accumulation of intermetallic compounds (IMC), such as Cu_6Sn_5, adversely impacts the solder joint toughness. Therefore, a basic understanding of the factors that determine the growth kinetics of IMC under distinct operating conditions is warranted to improve the reliability of microelectronic devices. However, predicting the growth of IMC involves tedious experiments or large-scale 3D phase-field simulations, both of which are labor- and resource-intensive techniques. Here, we present simple approaches that couple material thermodynamics with diffusional kinetics for predicting the isothermal growth characteristics of Cu_6Sn_5 in Cu-Sn alloy for temperatures ranging from 145°C to 230°C. While our calculations can reproduce the kinetics of growth obtained from experiments, they also indicate the limited role of IMC/Sn interfacial curvature in determining the rate at which the IMC layer thickens. The reported parametric study, while contrasting the uni- and bidirectional Cu_6Sn_5 growth rates, highlights the utility of combined thermodynamic-kinetic 1D approaches in predicting steady-state growth velocity of IMCs in Cu-Sn alloys.

Keywords Intermetallics · annealing · phase transformation · diffusion · joining

Introduction

With the rapid miniaturization of electronic circuits, thermal and mechanical loads on solder joints that provide the electrical connection between the substrate and the chip have increased. During the soldering process, a layer of intermetallic compound (IMC) is formed at the solder-substrate interface. Since this IMC layer is quite brittle, it can adversely impact the mechanical properties of the joint. In the subsequent aging process, the microstructure of the solder joint coarsens while the interface IMC layer thickens, resulting in stress concentration, promoting the nucleation and growth of cracks.[1-9] Additionally, the generation of Kirkendall voids within the IMC layer can significantly degrade the reliability of solder joints.[10, 11] Therefore, a fundamental knowledge of the morphological evolution of solder microstructure is essential for improving the reliability of the interconnects and for the optimization of the soldering processes.

In recent years, traditionally used Sn-Pb has increasingly been replaced by Pb-free Sn-rich solders. The composition of these solders, which offer an advantage of a higher melting point over Sn-Pb, range from eutectic to off-eutectic. Previous studies on isothermally solidified microstructures of eutectic Sn-rich alloys, while suggesting a competition between primary tetragonal Sn cells/dendrites and eutectic lamellae,[12] also indicate dominant kinetics of Cu_6Sn_5 when compared to Cu_3Sn, during the intermittent stages of growth.[13] Moreover, during the growth process, Cu_6Sn_5 retains a scalloped morphology.

The kinetics of uni- and bidirectional IMC growth has been a topic of several investigations in the past.[14-18] However, an accurate prediction is non-trivial given that several factors such as grain size and orientation, alloy composition, processing parameters such as the solder joint cooling rate, reflow temperature, and thermal aging time can influence the morphological evolution of IMCs. Temporal evolution of the scallop morphology and its thickness is a function of Sn grain size and texture, while Sn grain boundaries are known to act as preferential IMC nucleation sites. As the

✉ Kumar Ankit
kumar.ankit@asu.edu

[1] Materials Science and Engineering, School for Engineering of Matter, Transport and Energy, Arizona State University, 551 E. Tyler Mall, ERC 265, Tempe, AZ 85287, USA

[2] School of Materials Engineering, Purdue University, West Lafayette, IN 47906, USA

reflow proceeds, Cu_6Sn_5 scallops develop a crystallographic texture, which is related to FCC (face centered cubic) Cu. These scallops have both radial enlargement as well as perpendicular advancement when thermally aged at 240°C as shown in Fig. 1. The procedure adopted for reflowing, thermal aging, and characterization is described in our previous study.[17] Deng et al.,[16] reported that during thermal aging at 140–175°C the planarization of the scalloped morphology takes place owing to shorter diffusion distance between the Cu substrate and scallop valleys as opposed to the adjacent peaks. Here, a larger surface area of the scalloped surface, in comparison to the planar, provides the driving force for reduction in surface energy causing the diffusion of Cu from peaks to the valleys of scallops, which ultimately results in a planar growth front. A fast-cooling rate results in a planar scallop IMC growth front as opposed to slow cooling that favors the formation of scalloped surfaces which eventually planarize as the IMC growth proceeds. The incipient grooves provide more surface area for atomic diffusion when compared to a fully planar front. While the formation of Cu_6Sn_5 at the Cu-Sn interface is governed by the long-range diffusion of atoms in the bulk phase, i.e., Sn, or along the surface, the ripening fluxes that obey the Gibbs-Thompson rule cause coarsening of scallops, a process known to occur concurrently with IMC growth prior to the planarization of the surface. Beyond the factors specified above, applied tensile or compressive strains can also influence the growth process.[18-20]

As summarized above, the state-of-the-art techniques for predicting the IMC growth kinetics mostly rely on tedious experiments, which can be resource- and time-intensive. On the other hand, approaches that combine thermodynamic and kinetic modeling, such as Thermo-Calc when used in conjunction with diffusion-controlled transformations (DICTRA),[21, 22] can be leveraged for predicting the growth of IMCs. However, the combined approach still ignores the contribution of interfacial curvature and energy that can significantly influence microstructural evolution in solder joints. Although this issue is circumvented by coupling the CALPHAD (calculation of phase diagrams) approach with phase-field models,[23-29] the computational technique remains resource-intensive as several thousands of time steps must be simulated before the dynamic equilibrium can be attained, wherein the growth front traverses with a constant velocity. In the context of IMC growth, however, experimental observations infer that the scalloped IMC morphology planarizes before the steady-state velocity can be established. Therefore, leveraging this knowledge from literature, we hypothesize that one-dimensional DICTRA calculations that can compute the evolving concentration gradients during isothermal transformation should be able to yield sufficiently steady-state velocity of the IMC growth front. Therefore, the objective of this work is to validate the underlying hypothesis by analyzing the isothermal growth rates of Cu_6Sn_5 in Cu-Sn joints at distinct temperatures and comparing the findings with previous experimental results.

Integrating thermodynamic and kinetic approaches, which account for the role of concentration gradients and temperature, can potentially be an efficient alternative for predicting IMC growth rates in diffusion-limited regimes. With the aim of testing and validating such approaches, the following study analyzes the isothermal growth of planar Cu_6Sn_5 on the Cu-Sn composition and temperature. IMC growth rates obtained from simulations that leverage thermodynamic and kinetic databases are compared to the power laws observed in experimental studies for a range of temperatures. The rest of this paper is organized as follows. In "Methods" section, we revisit the theory underpinning the IMC growth, resulting microstructures, and the kinetics of Cu_6Sn_5 in a Cu-Sn diffusion couple. In "Results and Discussion" section, we explore the effectiveness of proposed computational approaches in predicting the kinetics of uni- and bidirectional Cu_6Sn_5 thickening for a range of temperatures. "Results" section concludes the article.

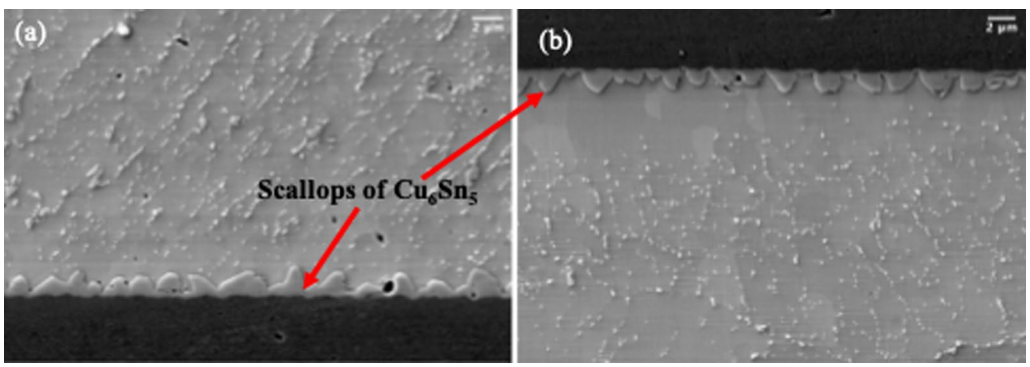

Fig. 1 Cu-Sn diffusion couple showing scallops of Cu_6Sn_5 formed at 230°C viewed at 3000x (a) Bottom surface (b) Top surface.

Methods

In "IMC Growth Mechanism" section the growth mechanism of the Cu_6Sn_5 intermetallic from various literature sources has been discussed in detail. In Sects. "Approch I" and "Approch II" sections, two different and innovative approaches are discussed for measuring this experimental growth rate via DICTRA. The diffusion model equations and the associated numerical techniques used for solving it have been reported earlier.[22] Finally, in "Bidirectional Growth Using Approach I" section, the growth rate of Cu_6Sn_5 has been measured for a Cu-Sn-Cu sandwich geometry and later compared with unidirectional Sn flow within the Cu region.

IMC Growth Mechanism

In general, Cu diffusion along the c-axis of Sn is known to be faster than the a-axis.[26, 27] Dyson et al.[32] reported that at low temperatures, the diffusivity of Cu along the c-axis direction is 500 times greater when compared to the a-axis and 10^{12} times greater than self-diffusivity of Sn at room temperature. It is to be noted that the ion core size of the diffusing element determines the magnitude of activation energy for interstitial diffusion. However, for substitutional diffusion, the electronic interaction of the diffusing species and vacancy plays a dominant role. At low temperatures, the radius of Cu atoms (1.25 Å) is consistent with the interstitial diffusion mechanism whereas at high temperature, i.e., when substitutional diffusion sets in, the Sn diffusion coefficient becomes comparable.

Following the nucleation of Cu_6Sn_5, the Sn diffusion coefficient in Cu_6Sn_5 ($D_{Sn} = 1.81 \times 10^{-17}$ m^2/s) exceeds that of Cu ($D_{Cu} = 0.76 \times 10^{-17}$ m^2/s) at 150°C. Since the Cu_6Sn_5 layer forms due to the presence of excess Cu, this layer grows much faster than Cu_3Sn and is present as the dominant IMC during thermal solidification.[33] The thickening rate of the Cu_6Sn_5 layer in a Cu-Sn diffusion couple is given by Eq. 1[29, 30]

$$H = Kt^n \tag{1}$$

where H is the thickness of interfacial IMC, K is a growth coefficient, t is the reaction time, and n is a time exponent. When the growth occurs in a grain boundary diffusion-controlled regime, $n = 0.33$, whereas it equals 0.5 and 1.0 for volume diffusion- and interface reaction-controlled regimes, respectively. Both the variants of IMC phases, namely, Cu_6Sn_5 and Cu_3Sn, that have been previously observed in isothermal growth experiments are known to be influenced by interdiffusion characteristics of Cu and Sn. These experiments have shown that below 170°C, the growth of IMC is governed by interstitial diffusion of Cu while vacancy diffusion of Sn dominates the growth process at higher temperatures. Apparently, these findings infer that below 170°C, Sn diffuses faster than Cu in Cu_6Sn_5.[30]

Based on phase-field calculations, Park and Arróyave[23] proposed the range, $0.21 < n < 0.34$, for concurrent growth and coarsening of IMCs. Deng et al.[16] resorted to three independent quenching techniques, namely, water, air, and furnace cooling, to explore the influence of cooling rate on the IMC growth rate and diffusional mechanisms. While the growth exponent, which was found to be in the range of 0.36–0.44 for the air-cooled sample, indicates the combined influence of diffusion fluxes arising from the bulk and along the grain boundaries, the former was found to be dominant in the furnace-cooled sample wherein the growth exponent ranged from 0.43 to 0.56. For furnace-cooling, the growth exponent was found to be 0.43 during the early stages of growth which indicates the predominance of grain boundary diffusion over bulk. However, formation of scallops led to curvature-driven coarsening which caused planarization of the growth front, thereby reducing the grain boundary area and leading to the bulk diffusion-controlled growth, as indicated by an increase of the exponent to 0.56. Based on the previous findings of Mannan et al.,[35] the CALPHAD models reported below assume that Cu_6Sn_5 growth at the Cu-Sn interface occurs when the local concentration of Cu exceeds the equilibrium value.

Approach I

To determine the isothermal growth of the Cu_6Sn_5 layer in a Cu-Sn diffusion couple, thermodynamic and kinetic databases for Cu-Sn solder alloys, namely, TCSLD3 and MOBSLD1, respectively, were leveraged. For obtaining the temporal displacement of the Cu_6Sn_5/Sn interface, we allocate a computational domain, as shown in Fig. 2a, which is representative of a Cu-Sn diffusion couple where the left region is assumed to be composed of pure Cu, while the one on the right corresponds to be a nearly pure Sn phase of composition, Sn-0.1 wt.% Cu.

To determine the temporally varying thicknesses of Cu_6Sn_5 as the Cu atoms progressively diffuse into the Sn region at elevated temperatures, the composition of Cu within the Sn-rich domain is continuously tracked. It is worth noting that our approach implicitly tracks the position of the Cu_6Sn_5/Sn interface by assuming that the IMC thickness at a given instant equals the distance at which Cu concentration falls below 39.1 wt.% within the Sn region, which is measured from the initial position of the Cu-Sn interface. To ensure long-range diffusion of Cu within Sn and to mitigate the effects of segregation that can lead to erroneous results, the width of the Sn-region is assumed to be 250 μm which is sufficiently long for allowing a smooth

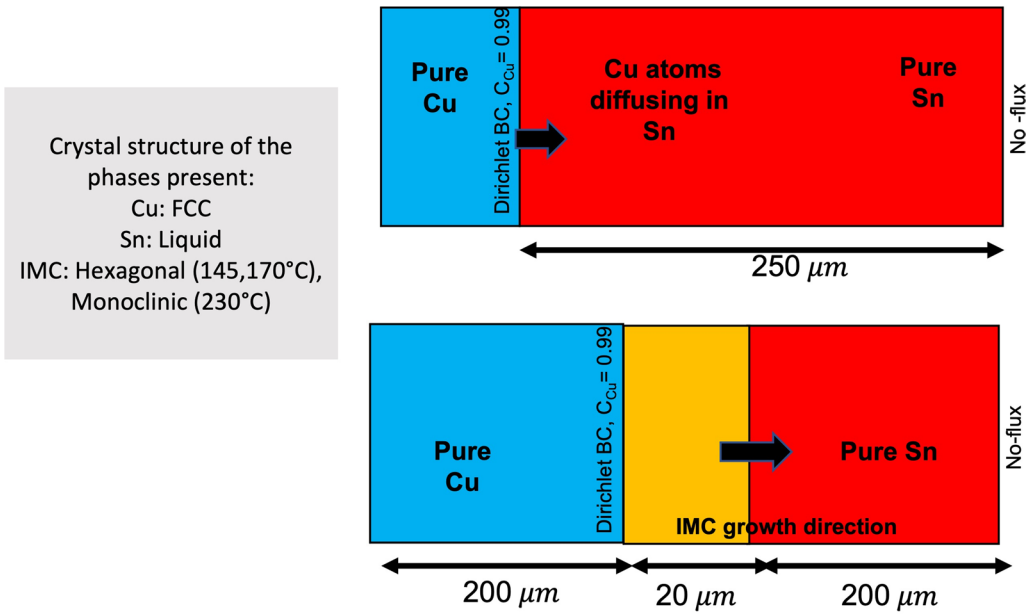

Fig. 2 Schematic representation of (a) pure Cu and pure Sn regions modeled using approach I, and (b) sandwich geometry comprising pure Cu, Cu_6Sn_5 (IMC), and pure Sn modeled using approach II. While compositional boundary conditions are imposed at the pure Cu/pure Sn and pure Cu/Cu_6Sn_5 interfaces, right domain edges are prescribed zero-flux. The Cu_6Sn_5/pure Sn interface (approach II) is modeled as a moving phase boundary such that local equilibrium conditions are maintained.

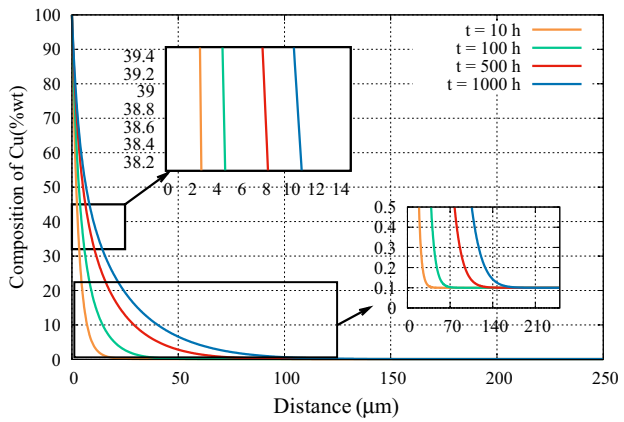

Fig. 3 Temporal evolution of Cu composition in pure Sn simulated using approach I.

concentration gradient to develop such that the Cu concentration approaches zero upon traversing from the left to the right edge, as seen in Fig. 3. Since our goal is to analyze the Cu_6Sn_5 growth kinetics that pertains to dynamic equilibrium, the temporal IMC thicknesses are measured for sufficiently long durations spanning 1000 h.

Approach II

In this second procedure, we introduce a 20-μm-wide layer of Cu_6Sn_5 sandwiched between Cu and Sn-rich regions, as shown in Fig. 2b. Expanding on the previous approach, Cu diffusion within the IMC is calculated as well as within pure Sn. The pure Cu (99.99 wt.% Cu and 0.01 wt.% Sn) region is assumed to be 200 μm wide to ensure a persistent supply of Cu atoms, whereas the width of the pure Sn (99.99 wt.% Sn and 0.01 wt.% Cu) region is varied in the range of 100–350 μm. Both approaches are used to deduce isothermal growth rates of Cu_6Sn_5 at temperatures ranging from 145°C to 230°C.

A major advantage of approach II is that it enables tracking of the Cu_6Sn_5/Sn interface as opposed to approach I were the temporal width of the Cu_6Sn_5 layer is implicitly deduced from the Cu composition plots. Applicability of both approaches is limited to 1D (one-dimension) while any contribution of interfacial diffusion has been completely ignored. Therefore, our approach is best suited for simulating those growth conditions where IMC thickening is governed by volumetric diffusion. Our sharp interface calculations reported below essentially rely on formation of a concentration gradient or presence of a solubility range (referenced from the phase diagram).[36] Despite being an IMC, availability of a small solubility range for Cu_6Sn_5 in the Cu-Sn phase diagram facilitates our 1D calculations which may otherwise need to be adapted for analyzing the growth of a line compound, such as Cu_3Sn that exhibits a negligible solubility range.

Bidirectional Growth Using Approach I

Here, we mimic the experimental conditions pertaining to a bidirectional evolution of Cu_6Sn_5, by using a set-up shown in Fig. 4, where Cu-rich regions enclose the Sn-rich region from both ends, while the entire set-up is isothermally held at distinct temperatures ranging from 145°C to 230°C. To better understand the influence of Sn-width and temperature on the bidirectional growth rate of Cu_6Sn_5, calculations are performed at distinct Sn widths of 100 µm, 250 µm, and 375 µm, at isothermal holding temperatures varying from 145°C to 230°C. Plots of growth rate corresponding to the bidirectional evolution of Cu_6Sn_5, obtained using approach I, are compared with the unidirectional growth of IMC. At this point, we would like to clarify that neither approach, being limited to 1D, encapsulates the effects of IMC/Sn interface irregularities that can arise during the reflowing of solders[37, 38] Therefore, the findings which are reported below mostly pertain to isothermal conditions where the IMC/Sn interfaces retain a planar morphology during growth.

Results and Discussion

In "Predicting the Growth of Cu_6Sn_5 Using Approaches I and II" section, we compare the unidirectional growth rates of Cu_6Sn_5 simulated using approaches I and II, respectively, with previously deduced power laws. We assess the influence of initial Cu_6Sn_5 widths and temperatures on the growth kinetics. In "Velocity of Cu_6Sn_5/Sn Transformation Front" section, we analyze the corresponding velocity of the Cu_6Sn_5/Sn front, while in "Comparison Between Unidirectional and Bidirectional IMC Growth", we contrast the unidirectional growth kinetics with the bidirectional evolution.

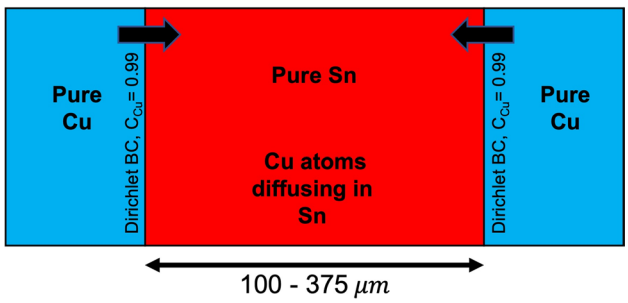

Fig. 4 Schematic representation of Cu-Sn diffusion couple for modeling bidirectional growth of IMC using approach I.

Predicting the Growth of Cu_6Sn_5 Using Approaches I and II

Figure 5a and b shows the temporal variation of Cu concentration within the Sn-rich region for temperatures 145°C and 170°C, respectively, simulated using approach I. The concentration gradient reduces over time as the Cu diffuses into the Sn-rich phase. The green and the yellow data points plotted in Fig. 5c are deduced based on approach I by leveraging the simulated concentration profiles corresponding to isothermal evolution at 145°C and 170°C. Both data sets obtained at distinct temperatures are found to be in reasonable agreement with the corresponding experimentally measured thicknesses of Cu_6Sn_5. Figure 5d and e shows composition profiles and temporal width of Cu_6Sn_5 for the isothermal transformation temperature corresponding to 230°C where Sn exists as melt.

The data corresponding to the temporal width of Cu_6Sn_5 at distinct temperatures upon fitting reproduce the well-known parabolic trend, as previously observed in experiments,[24, 33, 34] thereby validating our approach. We would like to clarify that modeling the clustering of atoms or the ensuing nucleation events are beyond the scope of the computational approaches discussed above. Thus, all of our IMC growth process simulations reported at distinct temperatures in this work proceed from a pre-existing Cu_6Sn_5 seed.

Plots in Fig. 6a, c, and e, compare Cu_6Sn_5 thicknesses obtained from approaches I and II with the experimental results in literature.[15] The same data, when plotted against the square root of isothermal solidification time, are found to scale linearly, which corroborates a parabolic growth trend, as shown in Fig. 6b, d, and f. At 140°C and 170°C, data obtained from approach I show better agreement with experiments as compared to II. However, convergence between these data with approach I and measured thicknesses is comparatively better at 230°C. In all certainties, this corroborates that the volume diffusion in the Sn region is the governing mechanism, while any diffusion within the IMC does not contribute to the growth kinetics of Cu_6Sn_5. The deviations observed with respect to the experimental data beyond 800 h and 100 h of reaction in Fig. 6c and e, respectively, is primarily due to the onset of coarsening of Cu_6Sn_5 scallops at elevated temperatures, the physics of which is not captured by any of the proposed approaches. Further, we would like to clarify that the diffusion coefficient within Sn melt (at 230°C) is larger than solid Sn (at 140°C and 170°C). Therefore, the primary diffusion mode simulated using our approach II automatically shifts to volume-controlled due to a large disparity in diffusion coefficients in the bulk Sn and growing IMC leading to a better agreement with approach I in Fig. 6c.

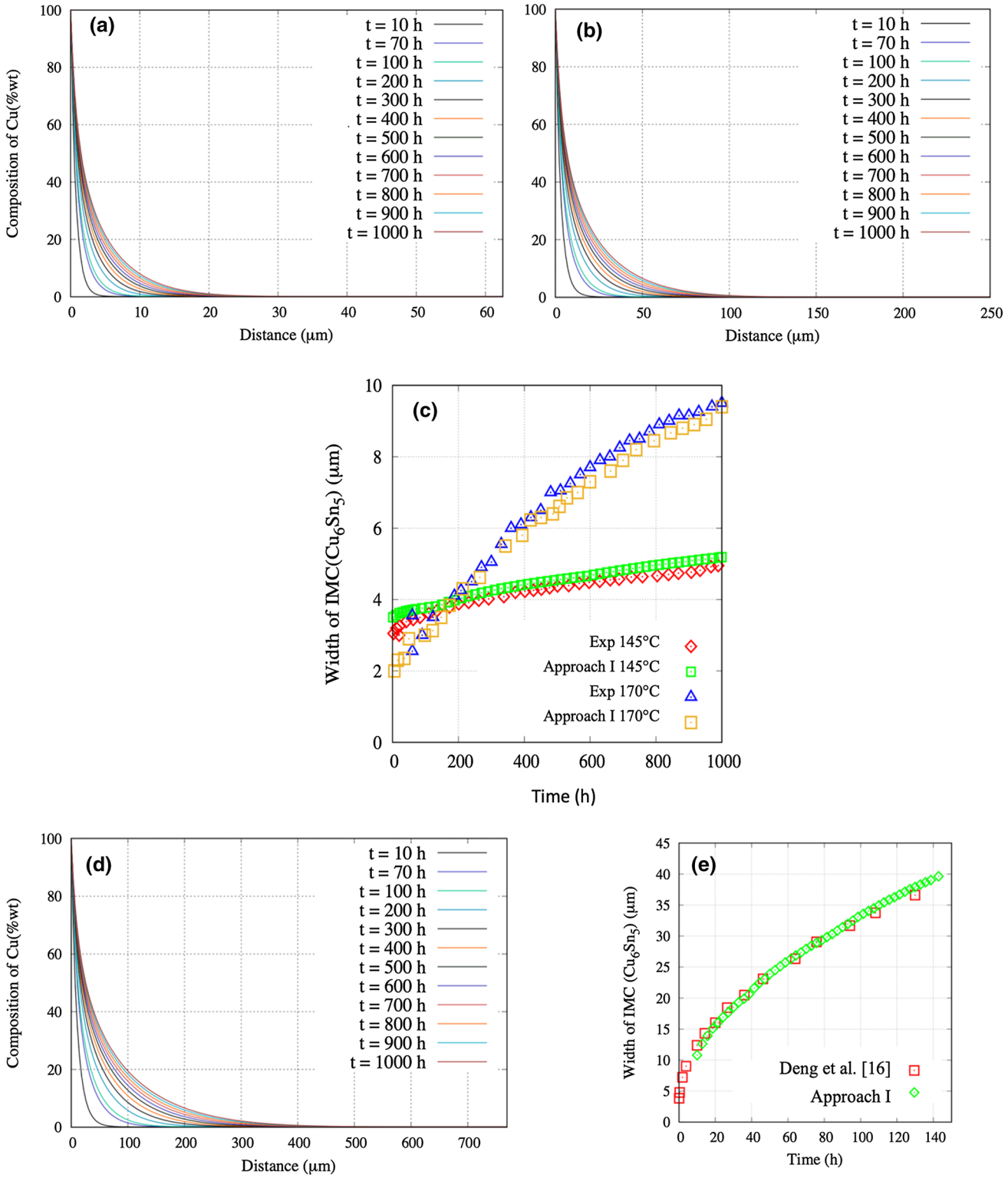

Fig. 5 Concentration profile of Cu plotted at representative time steps along the width of the Sn region at (a) 145°C (b) 170°C and (d) 230°C. Temporal widths of the Cu_6Sn_5 layer at isothermal holding temperatures 145°C and 170°C obtained from approach I are compared with experimental data in (c). A similar comparison of data sets for 230°C is shown in (e).

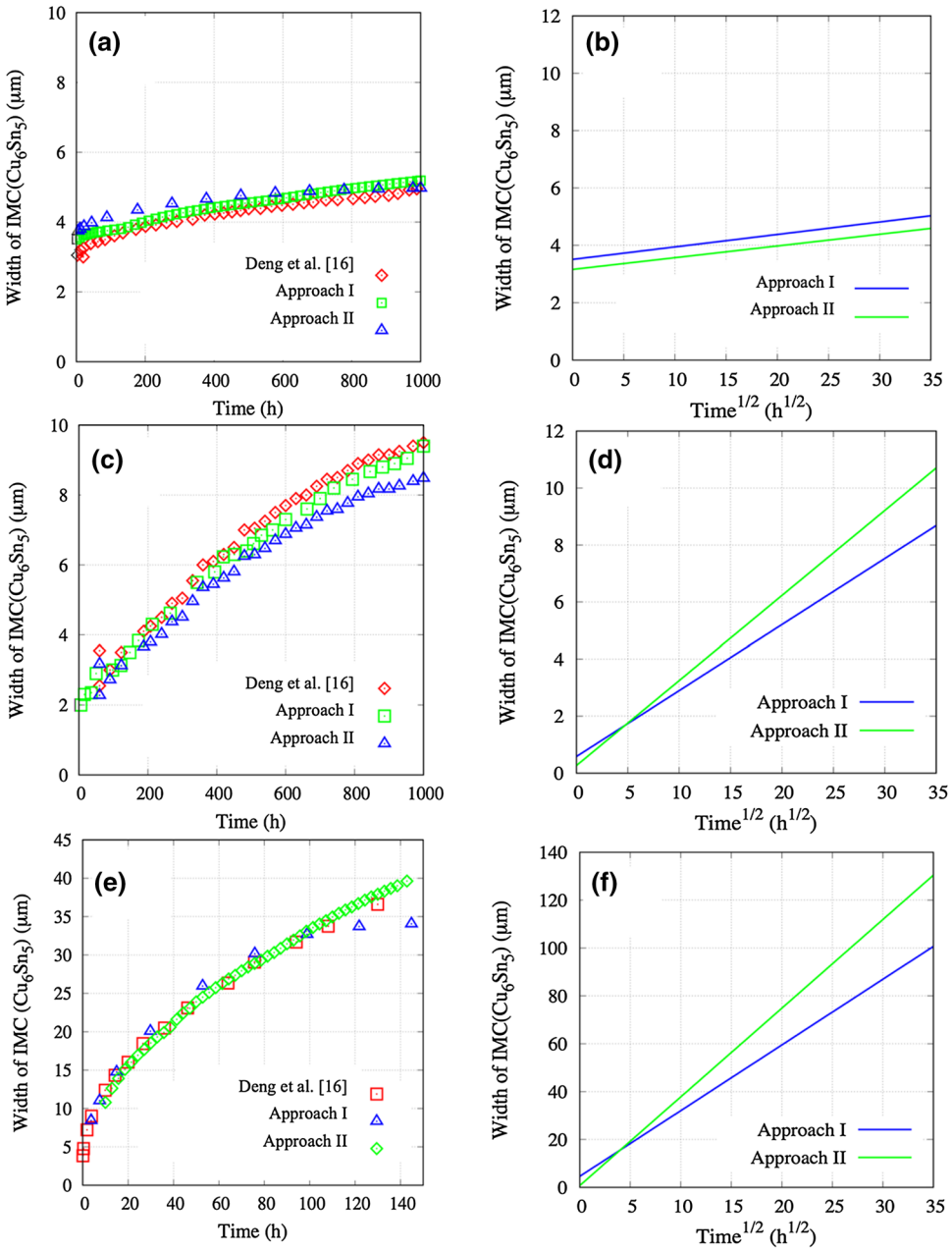

Fig. 6 Comparison of Cu_6Sn_5 growth kinetics obtained using approaches I and II with experiments at temperatures (a) 145°C (c) 170°C (e) 230°C. The simulated Cu_6Sn_5 layer thicknesses when plotted against square root of reaction time at (b) 145°C (d) 170°C (f) 230°C show a linear trend.

Velocity of Cu_6Sn_5/Sn Transformation Front

The proposed approaches, which couple materials thermodynamics with diffusional kinetics, ignore the influence of interface curvatures on the growth kinetics of Cu_6Sn_5. Based on this assumption, the rate of diffusion-controlled intermetallic growth is given by Refs. 8, 10, 35, 36

$$v = \frac{1}{C_{Sn/Cu_6Sn_5} - C_{Cu_6Sn_5/Sn}} \left(\tilde{D}_{Cu_6Sn_5} \frac{C_{Sn,Cu_6Sn_5}}{x_{Cu_6Sn_5}} - \tilde{D}_{Sn} \frac{C_{Sn,Sn}}{x_{Cu_6Sn_5}} \right) \quad (2)$$

where C_{Sn/Cu_6Sn_5} and $C_{Cu_6Sn_5/Sn}$ are equilibrium chemical compositions of the Sn and Cu_6Sn_5 phases as shown in Fig. 7, which are in contact with one another, whereas $\tilde{D}_{Cu_6Sn_5}$ and $\tilde{D}_{Sn}$ are the diffusion coefficients of Sn within Cu_6Sn_5, and pure Sn. Based on the parameters tabulated in Table I, corresponding velocity of the Cu_6Sn_5/Sn interface at 145°C is plotted in Fig. 7a. The plots in Fig. 7 compare the steady-state velocity of the Cu_6Sn_5/Sn interface simulated at 145°C and 170°C with experimentally measured ones that were reported earlier. At both temperatures, a temporal decrease in the Cu_6Sn_5 growth velocity is observed, as the transformation front attains a dynamic steady-state after approximately 7 h since the start of the reaction.

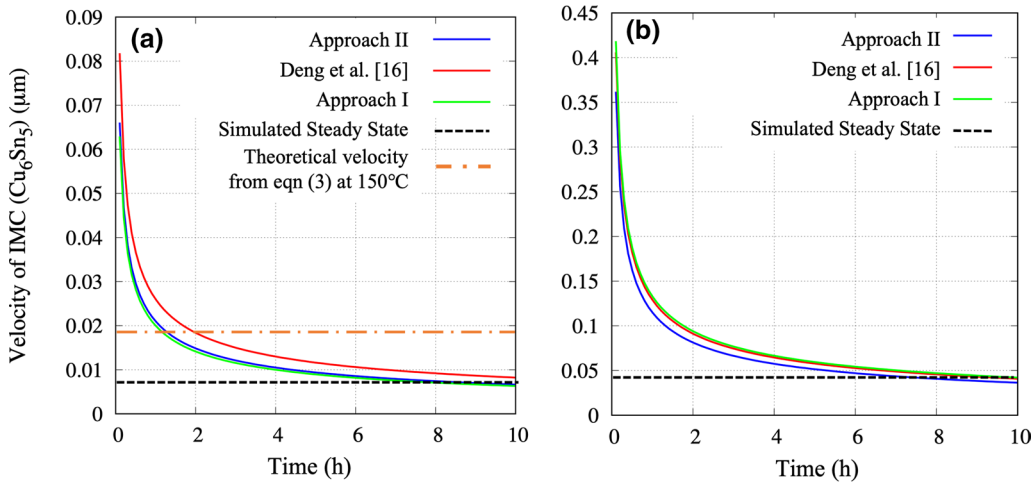

Fig. 7 Temporal velocity of the advancing Cu_6Sn_5 front at (a) 145°C (b) 170°C plotted using distinct approaches.

Table I Parameters for analyzing Cu_6Sn_5 layer thickening rate[31]

Parameters	Values
$D_{Sn}^{Cu_6Sn_5}$	6.11×10^{-16} m^2/sec
$D_{Cu}^{Cu_6Sn_5}$	5.56×10^{-16} m^2/sec
$\tilde{D}_{Cu_6Sn_5}$	5.86×10^{-16} m^2/sec
C_{Sn/Cu_6Sn_5}	0.99 at.% Sn
$C_{Cu_6Sn_5/Sn}$	0.1 at.% Sn
$\frac{\Delta C_{Sn,Cu_6Sn_5}}{\Delta x_{Cu_6Sn_5}}$	0.28 at.%/μm
$\frac{\Delta C_{Sn,Sn}}{\Delta x_{Cu_6Sn_5}}$	≈0 (from Fig. 6d)

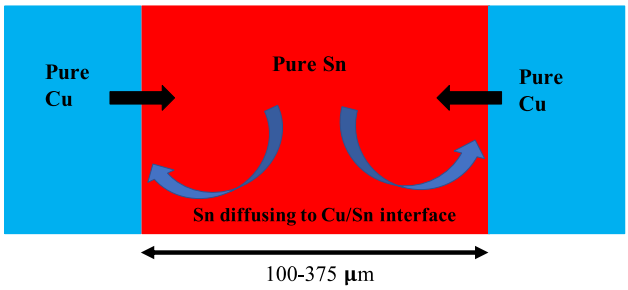

Fig. 8 A schematic diagram showing the diffusional fluxes of Cu and Sn atoms during bidirectional IMC growth.

Comparison Between Unidirectional and Bidirectional IMC Growth

To analyze the impact of overlapping diffusional fields in bidirectional growth, we adopt approach I to deduce and compare the growth rates on both ends of the diffusion couple, as shown by a schematic diagram in Fig. 8. Apparently, the extent of the overlap depends on the separation between the Cu-Sn interfaces at the opposite ends. Therefore, we plot temporal widths of Cu_6Sn_5 on the left and right edges in Fig. 9 for distinct lengths of this diffusion couple at isothermal transformation temperatures of 145°C, 170°C, and 230°C. This can be attributed to a smaller diffusion coefficient of Sn in the melt, unlike solid Sn, wherein overlapping diffusional fields do not alter the growth kinetics. However, the bidirectional growth rates, despite marginal differences with respect to the unidirectional, are found to obey the parabolic power law. In Fig. 9b and c, deviations from the experimental growth rates are observed below 50 h and 100 h, respectively, due to the formation of scallops with rounded interface, the physics of which is not captured by the current techniques. However, as the advancing transformation front planarizes over time, the simulated growth rates are found to converge with previous experimental results.

Conclusions

- The isothermal growth rates of Cu_6Sn_5 predicted by both approaches in the temperature range 145–230°C are found to be in reasonable agreement with previously measured rates.
- Based on the comparison of power laws, we can validate the underlying hypothesis that the steady-state velocity of the Cu_6Sn_5 growth front can be predicted using a 1D approach with an acceptable accuracy.
- Our study is also able to establish differences in the uni- and the bidirectional growth rates, thereby highlighting the influence of the length of the sandwiched pure Sn region on the kinetics of phase transformation.

Since both proposed approaches predict the growth rate solely based on the concentration gradient that drives the diffusion of atoms, we have implicitly assumed that

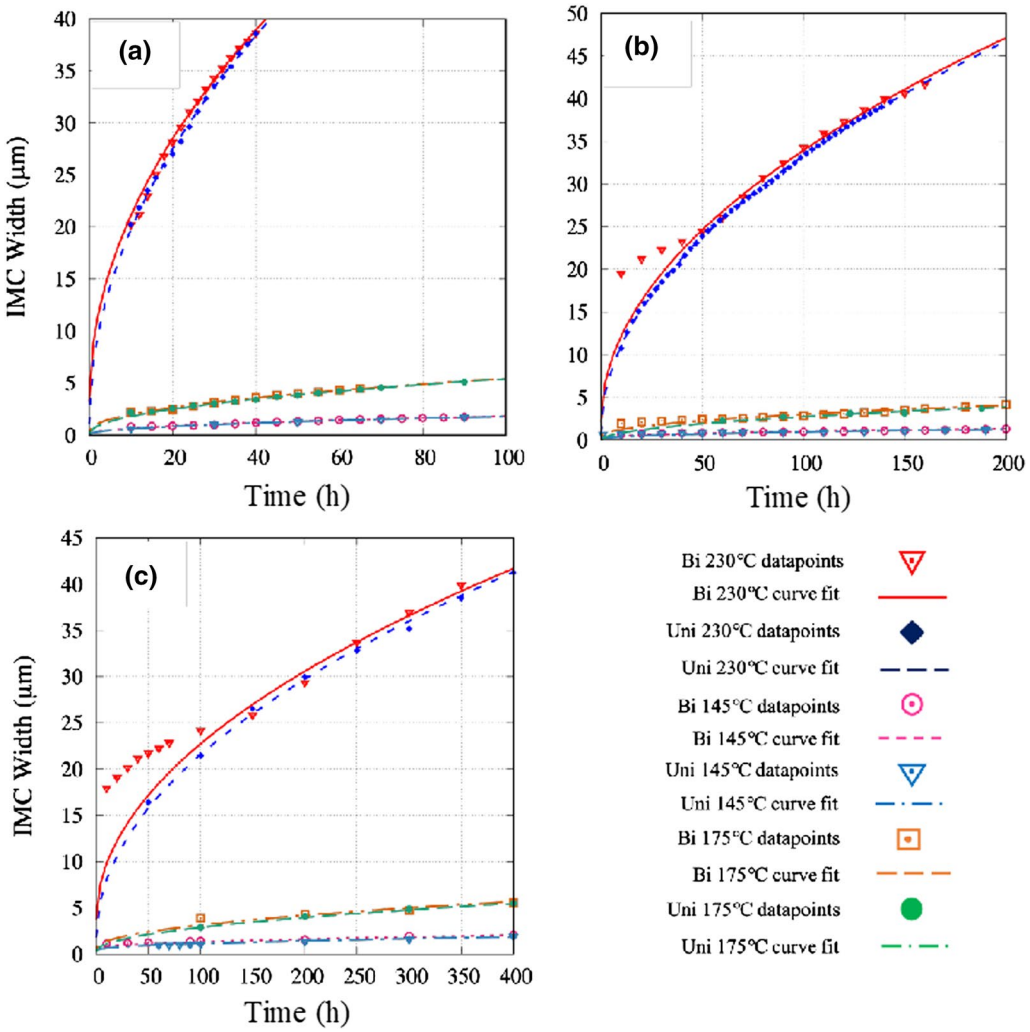

Fig. 9 Comparison of IMC growth rate for bidirectional and unidirectional growth in (a) 100 μm; (b) 250 μm; (c) 375 μm Sn bars.

the curvature of the scallops and interfacial energy do not influence the Cu_6Sn_5 growth rate. In other words, an important distinction between our calculations with previous experiments is that the former assumes that the growth proceeds from a seed with flat Cu_6Sn_5/Sn interface as opposed to actual growth, where starting from a seed, scallops form that ultimately planarize during transformation. However, the primary reason why the proposed approaches can predict the IMC growth kinetics with reasonable accuracy is because the time elapsed in achieving the steady-state velocity of the Cu_6Sn_5/Sn front is comparable to the overall duration over which scallops form and subsequently planarize. This allows us the liberty of ignoring the physics of curvature effects altogether in our calculations. Based on an agreement of simulated with previously measured values, we conclude that the Cu_6Sn_5/Sn interfacial curvature has little to no role in determining the growth kinetics, once the advancing Cu_6Sn_5/Sn front planarizes. The novelty of this work lies in our ability to predict the IMC growth rates accurately for a range of temperatures and growth conditions, despite coarse underlying assumptions related to 1D growth and interfacial energy, in a simplistic, yet high-throughput manner.

Acknowledgments The authors acknowledge financial support from the National Science Foundation (NSF) under Grant Nos. NSF CMMI-1763128 (Drs. Thomas Kuech and Alexis Lewis, Program Manager) and NSF AI Research Planning Grant—2020277 (Drs. John Schlueter, James Donlon, Rebecca Hwa, and Alexis Lewis Program Managers).

Funding National Science Foundation, 1763128, Kumar Ankit, 2020277, Kumar Ankit.

Conflict of interest
The authors declare that they have no conflict of interest.

References

1. M.Y. Guo, C.K. Lin, C. Chen, and K.N. Tu, Asymmetrical Growth of Cu 6Sn 5 Intermetallic Compounds Due to Rapid Thermomigration of Cu in Molten SnAg Solder Joints. *Intermetallics* 29, 155–158 (2012).
2. X. Liang, X. Li, P. Yao, Y. Li, and F. Jin, Interfacial Reaction During Fabricating of full Cu_3Sn Joints in Microelectronic Packaging. *Mater. Sci. Technol. (United Kingdom)* 33, 2024–2031 (2017).
3. N. Zhao, Y. Zhong, M.L. Huang, H.T. Ma, and W. Dong, Dissolution and Precipitation Kinetics of Cu_6Sn_5 Intermetallics in Cu/Sn/Cu Micro Interconnects Under Temperature Gradient. *Intermetallics* 79, 28–34 (2016).
4. J. Wang, C. Leinenbach, H.S. Liu, L.B. Liu, M. Roth, and Z.P. Jin, Re-assessment of Diffusion Mobilities in the Face-Centered Cubic Cu-Sn Alloys. *Calphad Comput. Coupling Phase Diagrams Thermochem.* 33, 704–710 (2009).
5. J. W. Xian, S. A. Belyakov, M. Ollivier, K. Nogita, H. Yasuda, and C. M. Gourlay, "Acta Materialia Cu 6 Sn 5 Crystal Growth Mechanisms During Solidi fi Cation of Electronic Interconnections," 126, 540–551, 2017.
6. N. Zhao, Y. Zhong, M.L. Huang, H.T. Ma, and W. Dong, Growth kinetics of Cu_6Sn_5 Intermetallic Compound at Liquid-Solid Interfaces in Cu/Sn/Cu Interconnects Under Temperature Gradient. *Sci. Rep.* 5, 1–12 (2015).
7. V. M. F. Marques, C. Johnston, and P. S. Grant, "Lead-Free Solders in Aerospace Applications," no. June, pp. 14–16, 2001.
8. E. George and M. Pecht, RoHS compliance in Safety and Reliability Critical Electronics. *Microelectron. Reliab.* 65, 1–7 (2016).
9. P.Y. Chia, A.S.M.A. Haseeb, and S.H. Mannan, Reactions in Electrodeposited Cu/Sn and Cu/Ni/Sn Nanoscale Multilayers for Interconnects. *Materials (Basel)* 9, 1–14 (2016).
10. B. Chao et al., Electromigration Enhanced Intermetallic Growth and Void Formation in Pb-Free Solder Joints. *J. Appl. Phys.* 100, 1–10 (2006).
11. D. Kim, J.H. Chang, J. Park, and J.J. Pak, Formation and Behavior of Kirkendall Voids within Intermetallic Layers of Solder Joints. *J. Mater. Sci. Mater. Electron.* 22, 703–716 (2011).
12. J.S. Kang, R.A. Gagliano, G. Ghosh, and M.E. Fine, Isothermal Solidification of Cu/Sn Diffusion Couples to form Thin-Solder Joints. *J. Electron. Mater.* 31, 1238–1243 (2002).
13. K.E. Yazzie et al., Growth kinetics of Cu_6Sn_5 Intermetallic Compound at Liquid-Solid Interfaces in Cu/Sn/Cu Interconnects Under Temperature Gradient. *Metall. Mater. Trans. A Phys. Metall. Mater. Sci.* 29, 55–64 (2011).
14. Y. Wang, Y. Yao, and L. Keer, An Analytical Model to Predict Diffusion Induced Intermetallic Compounds Growth in Cu-Sn-Cu Sandwich Structures. *Theor. Appl. Mech. Lett.* 10, 33–37 (2020).
15. X. Deng, G. Piotrowski, J.J. Williams, and N. Chawla, Influence of Initial Morphology and Thickness of Cu_6Sn_5 and Cu_3Sn Intermetallics on Growth and Evolution during Thermal Aging of Sn-Ag Solder/Cu Joints. *J. Electron. Mater.* 32, 1403–1413 (2003).
16. X. Deng, R.S. Sidhu, P. Johnson, and N. Chawla, Influence of Reflow and Thermal Aging on the Shear Strength and Fracture Behavior of Sn-3.5Ag Solder/Cu Joints. *Metall. Mater. Trans. A Phys. Metall. Mater. Sci.* 36A, 55–64 (2005).
17. K.E. Yazzie, J. Topliff, and N. Chawla, Communication: On the Asymmetric Growth Behavior of Intermetallic Compound Layers During Extended Reflow of Sn-Rich Alloy on Cu. *Metall. Mater. Trans. A Phys. Metall. Mater. Sci.* 43, 3442–3446 (2012).
18. C.P. Lin, C.M. Chen, and Y.W. Yen, Enhanced Growth of the Cu_6Sn_5 Phase in the Sn/Ag/Cu and Sn/Cu Multilayers Subjected to Applied Strain. *J. Alloys Compd.* 591, 297–303 (2014).
19. O.M. Abdelhadi and L. Ladani, Effect of Joint Size on Microstructure and Growth Kinetics of Intermetallic Compounds in Solid-Liquid Interdiffusion Sn3.5Ag/ cu-Substrate Solder Joints. *J. Electron. Packag. Trans. ASME* 135, 1–10 (2013).
20. C.P. Lin, C.M. Chen, C.H. Lin, and W.C. Su, Interfacial Reactions of Sn/Ag/Cu tri-Layer on a Deformed Polyimide Substrate. *J. Alloys Compd.* 502, 17–19 (2010).
21. J.O. Andersson, T. Helander, L. Höglund, P. Shi, and B. Sundman, Thermo-Calc & DICTRA, Computational Tools for Materials Science. *Calphad Comput. Coupling Phase Diagrams Thermochem.* 26, 273–312 (2002).
22. A. Borgenstam, A. Engstrom, L. Hoglund, and J. Agren, Basic and Applied Research: Section I DICTRA, a Tool for Simulation of Diffusional Transformations in Alloys. *J. Phase Equilibria* 21, 269–280 (2000).
23. M.S. Park and R. Arroyave, Formation and Growth of Intermetallic Compound Cu 6Sn 5 at Early Stages in Lead-Free Soldering. *J. Electron. Mater.* 39, 2574–2582 (2010).
24. M.S. Park, S.L. Gibbons, and R. Arróyave, Phase-Field Simulations of Intermetallic Compound Evolution in Cu/Sn Solder Joints Under Electromigration. *Acta Mater.* 61, 7142–7154 (2013).
25. K. Ankit, A. Choudhury, C. Qin, S. Schulz, M. McDaniel, and B. Nestler, Theoretical and Numerical Study of Lamellar Eutectoid Growth Influenced by Volume Diffusion. *Acta Mater.* 61, 4245–4253 (2013).
26. K. Ankit, R. Mukherjee, T. Mittnacht, and B. Nestler, Deviations from Cooperative Growth Mode During Eutectoid Transformation: Insights from a Phase-Field Approach. *Acta Mater.* 81, 204–210 (2014).
27. K. Ankit, T. Mittnacht, R. Mukherjee, and B. Nestler, Evolution of Mixed Cementite Morphologies During Non-cooperative Eutectoid Transformation in Fe – C Steels. *Comput. Mater. Sci.* 108, 1–6 (2015).
28. K. Ankit, R. Mukherjee, and B. Nestler, Deviations from Cooperative growth Mode During Eutectoid Transformation: Mechanisms of Polycrystalline Eutectoid Evolution in Fe–C Steels. *Acta Mater.* 97, 316–324 (2015).
29. A. Durga, P. Wollants, and N. Moelans, Phase-Field Study of IMC Growth in Sn–Cu/Cu Solder Joints Including Elastoplastic Effects. *Acta Mater.* 188, 241–258 (2020).
30. A. Paul, C. Ghosh, and W.J. Boettinger, Diffusion Parameters and Growth Mechanism of Phases in the Cu-Sn System. *Metall. Mater. Trans. A Phys. Metall. Mater. Sci* 42, 952–963 (2011).
31. S. Kumar, C.A. Handwerker, and M.A. Dayananda, Intrinsic and Interdiffusion in Cu-Sn System. *J. Phase Equilibria Diffus.* 32, 309–319 (2011).
32. B.F. Dyson, T.R. Anthony, and D. Turnbull, Interstitial Diffusion of Copper in Tin. *J. Appl. Phys.* 38, 3408 (1967).
33. D. Goyal, P. Liu, and A. Overson, A Comparison Study of Cu Dissolution Mechanism and Kinetics in Solder Joints under Electromigration and Extended Reflow. *Proc. Electron. Components Technol. Conf.* 2018, 440–447 (2018).
34. X. Liu, M. Huang, N. Zhao, and L. Wang, Liquid-State and Solid-State Interfacial Reactions Between Sn-Ag-Cu-Fe Composite Solders and Cu Substrate. *J. Mater. Sci. Mater. Electron.* 25, 328–337 (2014).
35. S. Mannan and M.P. Clode, Dissolution of Solids in Contact with Liquid Solder. *Solder. Surf. Mt. Technol.* 16, 31–33 (2004).
36. Y. Takaku, X.J. Liu, I. Ohnuma, R. Kainuma, and K. Ishida, Interfacial Reaction and Morphology Between Molten Sn Base Solders and Cu Substrate. *Mater. Trans.* 45, 646–651 (2004).
37. C. Dong et al., Investigation on Growth of the Orientation-Preferred Cu_6Sn_5 on (001)Cu During the Temperature-Increased Multiple Reflow Process. *J. Alloys Compd.* 885, 161205 (2021).
38. H.R. Ma et al., Evolution Behavior and Growth Kinetics of Intermetallic Compounds at Sn/Cu Interface During Multiple Reflows. *Intermetallics* 96, 1–12 (2018).